

A DFT and NBO Analysis of the Bonding in Titanocene Complexes containing a Five-membered L,L'-cyclic Ligand: L,L' = O,O'; S,S' or Se,Se'

Jeanet Conradie*

Department of Chemistry, University of the Free State, Bloemfontein 9301, South Africa

Received 4 August 2009, revised 2 February 2010, accepted 29 May 2010

ABSTRACT

An NBO analysis of the electron distribution in the DFT-optimized geometries of different $\text{Cp}_2\text{Ti}^{\text{IV}}(\text{L},\text{L}'\text{-BID})$ complexes with $\text{L},\text{L}'\text{-BID}$ = dioxolene, dithiolene or diselenolene, showed that a large degree of folding along the $\text{L}\cdots\text{L}$ axis is needed for sufficient $\text{Ti}\leftarrow\text{L}$ π -donation. The out of plane folding for maximum $\text{Ti}\leftarrow\text{L}$ π donation increases with larger Ti-L bond lengths: $\text{Cp}_2\text{Ti}^{\text{IV}}(\text{O},\text{O}'\text{-BID})$ ($\sim 35^\circ$) < $\text{Cp}_2\text{Ti}^{\text{IV}}(\text{S},\text{S}'\text{-BID})$ (47° average) < $\text{Cp}_2\text{Ti}^{\text{IV}}(\text{Se},\text{Se}'\text{-BID})$ (50° average).

KEYWORDS

Gaussian, NBO, titanocene.

1. Introduction

Titanocene dichloride, $\text{Cp}_2\text{Ti}^{\text{IV}}\text{Cl}_2$ (Cp = cyclopentadienyl, $\eta^5\text{-C}_5\text{H}_5$), is widely used in organometallic and organic synthesis both as a reagent and as a catalyst.¹ Free titanocene, Cp_2Ti , is a 14 electron species and is not isolable. However, a wide range of stable 16 electron Ti(IV) complexes of the type $\text{Cp}_2\text{Ti}^{\text{IV}}(\text{BID})$ where BID is a potentially bidentate ligand, exists.² The chemical reactivity of these complexes is largely determined by the relative frontier orbital energies.³ The frontier molecular orbitals (MOs) of the bent $\text{Cp}_2\text{Ti}^{2+}$ fragment are described by Lauher and Hoffmann⁴ as 1a_1 (LUMO), b_2 (LUMO+1), 2a_1 (LUMO+2), b_1 (LUMO+3) and a_2 (LUMO+4) under C_{2v} symmetry (see Fig. 1).

Folding along the $\text{S}\cdots\text{S}$ hinge of the metallacycle in Cp_2Ti (dithiolene) complexes resulted in a stabilizing interaction between the empty acceptor LUMO 1a_1 orbital of the $\text{Cp}_2\text{Ti}^{2+}$ fragment and the HOMO (a π orbital of b_1 symmetry) of the dithiolene ligand.⁴ This stabilizing interaction is only possible if there is a symmetry lowering of the Cp_2Ti (dithiolene) complex and associated folding of the TiS_2C_2 metallacycle with bending values θ well above 40° ,⁵ as illustrated in Fig. 2. Similar folding is observed in Cp_2Ti (dioxolene)⁶ and Cp_2Ti (diselenolene)⁷ complexes.

Density functional theory (DFT) has become the method of choice for computational studies of medium-sized molecules.⁸ In this study we use the DFT approach to further understand the Ti-ligand bond and orbital mixing in a series of $\text{Cp}_2\text{Ti}^{\text{IV}}(\text{L},\text{L}'\text{-BID})$ complexes with $\text{L},\text{L}'\text{-BID}$ = dianionic bidentate ligand with donor atoms L and L' containing different donor/acceptor properties, viz. $\text{L},\text{L}' = \text{O},\text{O}'$; S,S' or Se,Se' . An NBO analysis quantifies the degree of the $\text{Ti}\leftarrow\text{ligand}$ π -charge transfer.

2. Theoretical Approach

Density functional theory (DFT) calculations were carried out using the GAUSSIAN 03 program⁹ with the PW91 exchange and correlation functional.¹⁰ Optimizations were done in the gas phase with the 6-311G(d,p) basis set on all atoms. A spin-restricted formalism was used. The accuracy of the computational method was evaluated by comparing the root-mean-

square (RMS) deviation between the optimized molecular structure and the crystal structure, using the non-hydrogen atoms in the molecule. RMS deviation values were calculated using the 'RMS Compare Structures' utility in ChemCraft Version 1.5.¹¹ Whether artificially generated atomic coordinates, or coordinates obtained from X-ray crystal data were used in the input files, optimizations for each compound resulted in the same minimum energy optimized geometry. Optimized structures were verified as a minimum through frequency calculations. Unless indicated, no symmetry limitations were imposed on the calculations. Geometries obtained from DFT calculations were used to perform an NBO analysis by using the NBO 3.1 module¹² in GAUSSIAN 03.⁹

3. Results and Discussion

Density functional theory (DFT) calculations were carried out on the series of $d^0 \text{Cp}_2\text{Ti}^{\text{IV}}(\text{L},\text{L}'\text{-BID})$ complexes containing a five-membered L,L'-cyclic ligand with $\text{L},\text{L}' = \text{O},\text{O}'$; S,S' or Se,Se' , with known crystal structures in order to validate the reliability of the computational method used. Selected calculated and experimental geometrical parameters of these $\text{Cp}_2\text{Ti}^{\text{IV}}(\text{L},\text{L}'\text{-BID})$ complexes are presented in Table 1. The validity of the density functional method is obtained by comparing the calculated data with the known single crystal X-ray diffraction structural data of these complexes. The root-mean-square distance (RMSD) values calculated for non-hydrogen atoms for the best three-dimensional superposition of calculated structures on experimental structures give a qualitative measurement of the accuracy of the ground state geometries of the calculated structures. Excellent agreement between experimental and theoretical structures was obtained as reflected by the RMSD values less than 0.02 Å, except for the $\text{Cp}_2\text{Ti}^{\text{IV}}$ (benzil-O,O') complex with a RMSD value of 0.46 Å. The large RMSD value of $\text{Cp}_2\text{Ti}^{\text{IV}}$ (benzil-O,O') is a result of the rotation of the Cp rings in the optimized complex relative to the experimental structure. All the bonds in the Ti-L,L' ring structure of the different $\text{Cp}_2\text{Ti}^{\text{IV}}(\text{L},\text{L}'\text{-BID})$ complexes in Table 1 were reproduced by DFT calculations within 0.02 Å for Ti-L bonds, within 0.03 Å for L-C bonds and within 0.01–0.04 Å for C-C bonds from the experimental values. Since comparisons of

* E-mail: conradj@ufs.ac.za

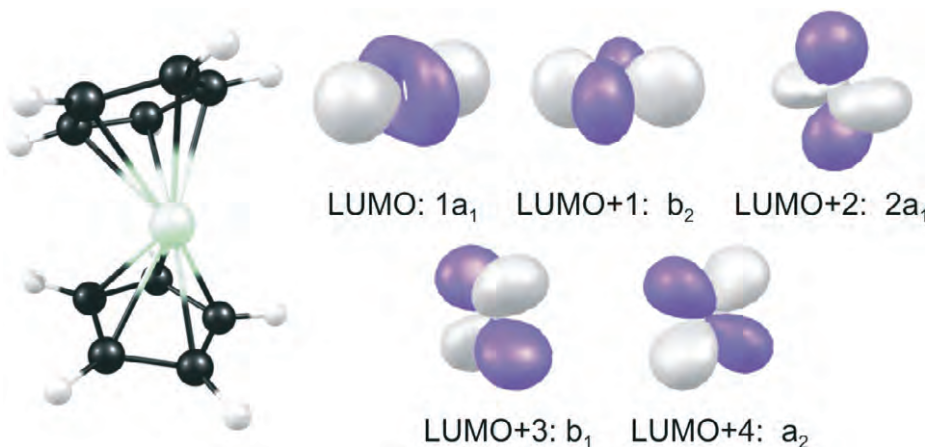


Figure 1 DFT Kohn-Sham MO presentations of the five important frontier MOs (right) of the bent $\text{Cp}_2\text{Ti}^{2+}$ fragment (left) under a C_{2v} symmetry constraint.

experimental metal-ligand bond lengths with calculated bond lengths below a threshold of 0.02 Å are considered as meaningless,¹³ the computational method used therefore gives an excellent account of experimental bond lengths. The L-Ti-L' angles were calculated accurately within 1.1°. DFT-optimized structures containing titanocene with the Cp rings in the staggered or in the eclipsed conformation are approximately equi-energetic, with no preference for either conformation. Especially pleasing is the fact that all the models optimized spontaneously to C_s symmetry around the metal centre in agreement with the experimental crystal structures. The folding around the L,L'-axis, measured by the angle θ between the plane through the Ti-L-L' atoms and the plane through the L'-L-C-C' atoms (Fig. 2), is reproduced by the DFT calculations within 1.1°. The increasing order of experimental bending angle θ around the L,L'-axis in going from $\text{Cp}_2\text{Ti}^{\text{IV}}(\text{O},\text{O}'\text{-BID})$ (~35°) to $\text{Cp}_2\text{Ti}^{\text{IV}}(\text{S},\text{S}'\text{-BID})$ (48° average) to $\text{Cp}_2\text{Ti}^{\text{IV}}(\text{Se},\text{Se}'\text{-BID})$ (50° average) is also well reproduced by the DFT calculations.

The $\text{Cp}_2\text{Ti}^{\text{IV}}(\text{L},\text{L}'\text{-BID})$ complexes are formally 16-electron d^0 complexes if only Ti-L σ -bonding is considered. The Kohn-Sham molecular orbitals (MOs) of simplified $\text{Cp}_2\text{Ti}^{\text{IV}}(\text{L},\text{L}'\text{-BID})$ models, *viz.* $\text{Cp}_2\text{Ti}(\eta^2\text{-LC(CH}_3\text{)}=\text{C(CH}_3\text{)L})$ ($\text{L} = \text{O, 1, S, 2, or Se, 3}$) with a C_s symmetry constraint were constructed to investigate how the orbital mixing looks for these complexes. The ordering and character of the frontier MOs of the simplified models **1–3** are very similar. Figures S1 and S2 of the supplementary material give presentations of a number of MOs of **1–3**, including the MOs of the free ligands (optimized geometries) associated with these complexes. All the complexes are stabilized by the expected σ -type interactions between the $\text{Cp}_2\text{Ti}^{2+}$ fragment and

the L,L'-BID fragment. For example for $\text{Cp}_2\text{Ti}(\eta^2\text{-SeC(CH}_3\text{)}=\text{C(CH}_3\text{)Se})$, **3**, the filled HOMO-2 of the ligand of symmetry a_1 donates electron density into the empty $2a_1$ LUMO+2 fragment MO of $\text{Cp}_2\text{Ti}^{2+}$ to form the α HOMO-4 of the complex. The filled HOMO-1 of the ligand of symmetry b_2 donates electron density into the empty b_2 LUMO+1 fragment MO of $\text{Cp}_2\text{Ti}^{2+}$ to form the α HOMO-3 of the complex. A presentation of the MOs involved in these Ti-L σ interactions is given in Fig. 3.

Out of plane π -type interactions involving the $1a_1$ LUMO of the $\text{Cp}_2\text{Ti}^{2+}$ fragment and the b_1 HOMO of the ligand, as illustrated schematically in Fig. 2, are observed in the HOMO of all three complexes. The electron count for these formally 16-electron complexes is increased by Ti-L π donation (see Fig. 3 for the HOMO of **3** to visualize the Ti-L π interaction). This interaction in $\text{Cp}_2\text{Ti}(\text{dioxolene})$ and $\text{Cp}_2\text{Ti}(\text{diselenolene})$ calculated with DFT in this study, is similar to the interaction described earlier on the basis of EH calculations, for 5-membered metallacycle $\text{Cp}_2\text{Ti}(\text{dithiolene})$ complexes.^{4,5}

The bond energies, ΔE , of the Ti-L bonds provide a good approximation to bond strength values.¹⁴ ΔE is the energy associated with the interaction between the two fragments $\text{Cp}_2\text{Ti}^{2+}$ and $(\text{L},\text{L}'\text{-BID})^{2-}$, which both possess the local equilibrium geometry of the final molecule, and which both have an electronic structure suitable for bond formation.¹⁵ The bond energy values of the Ti-L bonds of the different $\text{Cp}_2\text{Ti}^{\text{IV}}(\text{L},\text{L}'\text{-BID})$ complexes calculated with DFT in this study are tabulated in Table 1. The calculated values show that for the simplified models:

$$\begin{aligned} &\Delta E \text{ Cp}_2\text{Ti}(\eta^2\text{-OC(CH}_3\text{)}=\text{C(CH}_3\text{)O}) (-2571 \text{ kJ mol}^{-1}) < \\ &\Delta E \text{ Cp}_2\text{Ti}(\eta^2\text{-SC(CH}_3\text{)}=\text{C(CH}_3\text{)S}) (-2204 \text{ kJ mol}^{-1}) < \\ &\Delta E \text{ Cp}_2\text{Ti}(\eta^2\text{-SeC(CH}_3\text{)}=\text{C(CH}_3\text{)Se}) (-2179 \text{ kJ mol}^{-1}); \\ &d(\text{Ti-O}) (1.966 \text{ \AA}) < d(\text{Ti-S}) (2.415 \text{ \AA}) < d(\text{Ti-Se}) (2.557 \text{ \AA}); \\ &\theta \text{ Cp}_2\text{Ti}(\eta^2\text{-OC(CH}_3\text{)}=\text{C(CH}_3\text{)O}) (40.5^\circ) < \\ &\theta \text{ Cp}_2\text{Ti}(\eta^2\text{-SC(CH}_3\text{)}=\text{C(CH}_3\text{)S}) (44.9^\circ) < \\ &\theta \text{ Cp}_2\text{Ti}(\eta^2\text{-SeC(CH}_3\text{)}=\text{C(CH}_3\text{)Se}) (48.6^\circ). \end{aligned}$$

Thus the bond energy, ΔE , is the strongest for **1**, which has the shortest Ti-L bond length. More folding is possible for **2** and **3** with longer Ti-L bond lengths in order to get the largest bond strength possible for these complexes. The experimental systems show the same trend.

The Ti-L bond energy, ΔE , the total energy and the corresponding Ti-L bond length as functions of the folding angle, θ , around the L,L'-axis for the simplified models **1–3**, are illustrated in Fig. 4. For both complexes $\text{Cp}_2\text{Ti}(\eta^2\text{-SC(CH}_3\text{)}=\text{C(CH}_3\text{)S})$, **2**, and

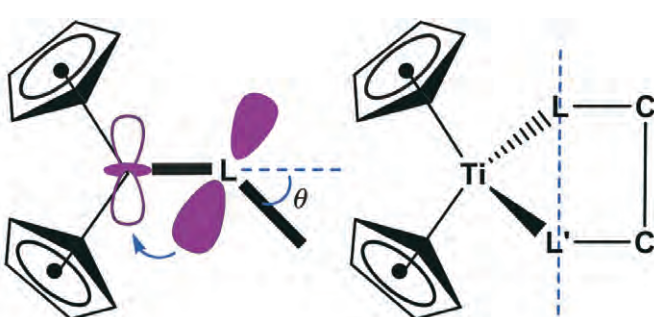


Figure 2 Folding angle, θ , around the L,L'-hinge in $\text{Cp}_2\text{Ti}(\text{L},\text{L}'\text{-BID})$ compounds leads to symmetrical out of plane Ti($1a_1$) – L(π) interaction (left) as observed in $\text{Cp}_2\text{Ti}(\text{dithiolene})$ complexes.⁵ θ is defined as the angle between the plane through the Ti-L-L' atoms and the plane through the L'-L-C-C' atoms (right).

Table 1. Selected NPA charge, bond energy of the Ti-L bond and geometrical parameters for the indicated experimental $\text{Cp}_2\text{Ti}(\text{L}-\text{BID})$ compounds (optimized with no symmetry constraint) as well as the simplified models **1-3** (optimized with C_s symmetry constraint).

	d(Ti-L) Å	d(Ti-L)/Å	d(L-C) Å	d(L'-C) Å	d(C-C) Å	$\frac{\theta}{\theta^\circ}$	RMSD Å	ΔE/kJ mol⁻¹	q(Ti)/e	q(L)/e	Ref.
	exp	calc	exp	calc	exp	exp	calc	calc	calc	calc	
0.0°											
Cp ₅ O ₂	-	1.966	-	1.966	-	1.349	-	1.349	-	40.5	-
Cp ₅ O ₂ Ph	1.965	1.967	1.960	1.954	1.361	1.341	1.337	1.349	1.407	81.8	81.2
S,S'	-	2.415	-	2.415	-	1.758	-	1.758	-	44.9	-
Cp ₅ S ₂	2.418	2.428	2.411	2.417	1.736	1.766	1.764	1.766	1.410	1.431	81.9
Cp ₅ S ₂ Ph	2.430	2.442	2.404	2.428	1.737	1.743	1.741	1.742	1.342	1.370	83.2
S ₂	2.435	2.453	2.430	2.446	1.733	1.737	1.717	1.736	1.357	1.392	84.4
S ₂ Ph	2.412	2.428	2.416	2.438	1.733	1.751	1.735	1.743	1.374	1.389	82.5
AVERAGE ^c	2.424	2.438	2.415	2.432	1.735	1.749	1.739	1.747	1.371	1.395	83.0
Se,Se'	-	2.557	-	2.557	-	1.929	-	1.929	-	82.5	-
Cp ₅ Se ₂	2.546	2.552	2.560	2.564	1.908	1.919	1.909	1.920	1.407	1.423	82.1
Cp ₅ Se ₂ Ph	2.568	2.579	2.533	2.528	1.879	1.893	1.898	1.911	1.363	1.378	82.6
Cp ₅ Se ₂ CO ₂ CH ₃	2.548	2.576	2.555	2.543	1.895	1.901	1.902	1.909	1.369	1.379	82.6
AVERAGE ^c	2.554	2.569	2.546	2.548	1.894	1.904	1.903	1.913	1.380	1.393	82.4

RMSD values, in Å, are root mean square atom positional deviations, calculated for non-hydrogen atoms for the best three-dimensional superposition of calculated structures on experimental structures.

REMD values of m_{ij} are mean square atom position deviation

ΔE is the calculated bond energy or the ΣE bonds in kJ/mol.

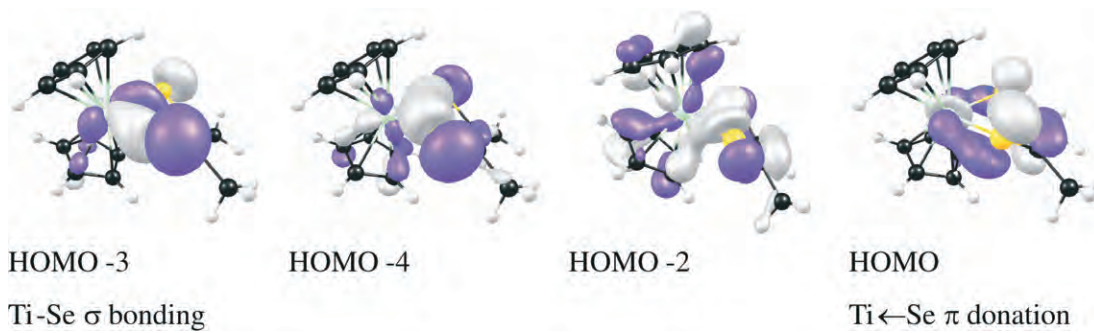


Figure 3 Selected occupied MOs of $\text{Cp}_2\text{Ti}(\eta^2\text{-SeC}(\text{CH}_3)=\text{C}(\text{CH}_3)\text{Se})$, 3. The b_2 type (HOMO-3) and the $2a_1$ type MO (HOMO-4) showed $\text{Ti} \leftarrow \text{L} \sigma$ interactions. The HOMO showed $1a_1 - \pi$ interaction with the b_1 HOMO of the ligand, made possible by symmetry lowering of the complex. A contour of $0.05 e \text{ Å}^{-3}$ has been used for the orbital plots.

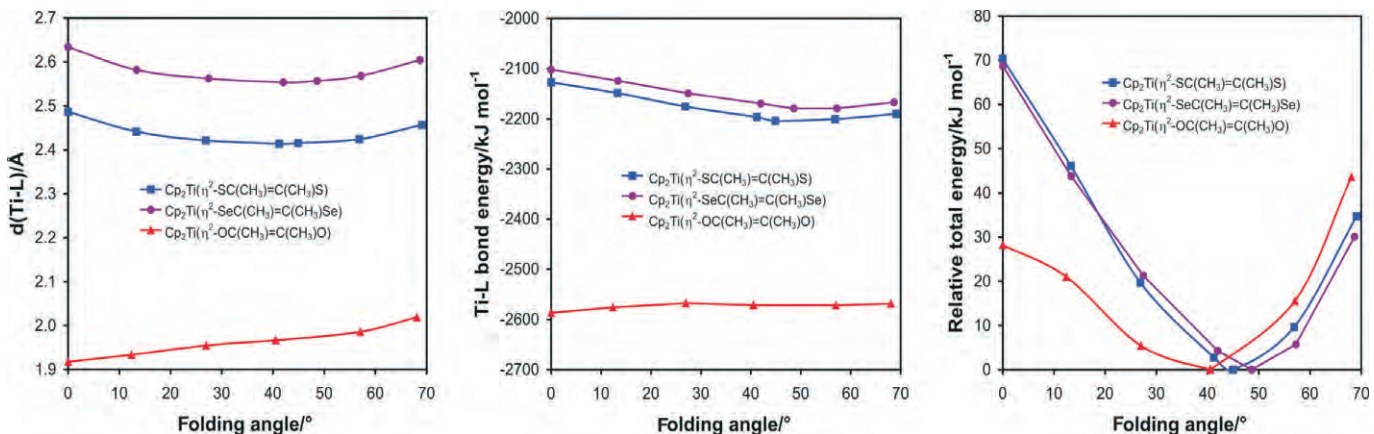


Figure 4 Bond length, Ti-L bond energy and relative total energy as functions of the folding angle, θ , for the simplified models $\text{Cp}_2\text{Ti}(\eta^2\text{-LC}(\text{CH}_3)=\text{C}(\text{CH}_3)\text{L})$, L = O, S or Se (optimized with C_s symmetry constraint).

$\text{Cp}_2\text{Ti}(\eta^2\text{-SeC}(\text{CH}_3)=\text{C}(\text{CH}_3)\text{Se})$, 3, the shortest Ti-L bond length as well as the most negative Ti-L bond energy (greatest bond strength) correspond to the most stable geometry (minimum total energy). Regarding $\text{Cp}_2\text{Ti}(\eta^2\text{-OC}(\text{CH}_3)=\text{C}(\text{CH}_3)\text{O})$, 1, we observe that the total energy curve as a function of the folding angle is very soft; the $\theta = 0^\circ$ geometry is only 28 kJ mol^{-1} less stable than the minimum energy geometry, compared with $68\text{--}70 \text{ kJ mol}^{-1}$ for 2 and 3. The difference in the Ti-L bond energy between the $\theta = 0^\circ$ and the minimum energy geometry of 1 is even less, 15 kJ mol^{-1} , compared with *ca.* 77 kJ mol^{-1} for 2 and 3.

In order to analyze and compare the electron distribution density in $\text{Cp}_2\text{Ti}^{IV}(\text{L,L'-BID})$ complexes with $\text{L,L'-BID} =$ dioxolene, dithiolene or diselenolene quantitatively, natural population analysis (NPA) and natural bond orbital (NBO) analyses were performed on the simplified models 1–3. The magnitude of the natural atomic charge on L of the L,L'-BID ligand (L = O, S or Se) gives evidence of the degree of π -bonding from the lone pairs on L to the empty Ti-d orbitals: $-0.627 e$ (O) $< -0.089 e$ (S) $\leq -0.046 e$ (Se) (see Table 1). This indicates that the $\text{Ti}_d \leftarrow \text{L}_p \pi$ -bonding in complex 1 is weaker than in complexes 2 and 3. This is in agreement with a smaller natural atomic charge on Ti for 2 and 3, $1.312 e$ (O) $> 0.999 e$ (S) $\approx 1.003 e$ (Se) (see Table 1); a more electron-deficient titanium centre will have a larger extent of π -bonding.¹⁶ This order is the same as the increasing order of the folding of complexes 1–3. A longer Ti-L bond length allows for a greater folding before the L,L'-BID ligand collides with the cyclopentadienyl ligand. It is expected that complexes with a larger degree of folding need a larger degree of $\text{Ti}_d \leftarrow \text{L}_p \pi$ -bonding between the empty acceptor LUMO $1a_1$ orbital of the $\text{Cp}_2\text{Ti}^{2+}$ fragment and the HOMO $b_1 \pi$ orbital of the L,L'-BID ligand for the same Ti-L bond energy. Exactly the same

trend concerning the natural atomic charge in the L-p orbitals, the natural atomic charge on Ti, the Ti-L bond length or the degree of folding was observed experimentally for the real complexes (see Table 1).

To explore the electron density of the NBO from a single complex perspective to eliminate steric effects of the coordinating atom L, the natural charges as a function of folding angle for complexes 1–3 are given in Table 2. For both complexes 2 and 3, the minimum (positive) natural charge on Ti and the minimum (negative) natural charge on L correspond to the minimum energy geometry. This implies that the bending of complexes 2 and 3 is optimal for maximum π -bonding from the lone pairs on L to the empty Ti-d orbitals. Complex 1 did not follow this trend.

The basic parameters of the natural orbitals of bonds and lone electron pairs (LPs) which involve the L (L = O, S or Se) and titanium atoms for 1–3 are listed in Table 3. For each O atom in 1 one natural O-C bond orbital and three lone pair orbitals were detected. For each L atom in 2 (L=S) and 3 (L=Se) one natural L-C bond orbital, one natural Ti-L bond orbital and two lone pair orbitals were detected. Due to C_s symmetry the NBOs on L and L' have the same character.

Each L-C NBO is a 2-centre bond (BD) with a population of 1.983, 1.972 and 1.965 e for 1–3, respectively, showing small deviations from an ideal Lewis structure. The O-C NBO of 1 has *ca.* 66 % O character and 34 % C character and is polarized towards the oxygen atom because O has a higher electronegativity.¹⁷ The S-C and Se-C NBOs of 2 and 3 are less polarized, which is in agreement with the similar electronegativities of S, Se and C. Figure 5 (middle row) gives a visualization of the bonding and antibonding O-C and Se-C NBOs.

No natural Ti-O bond orbital was detected for 1. The natural

Table 2 Selected NPA charges, bond energies of the Ti-L bond and geometrical parameters for the simplified models **1–3** (optimized with C_s symmetry constraint) as a function of folding angle, θ .

Complex	Dihedral angle Ti-L-C-C' /°	Folding angle, θ /°	d(Ti-L)/Å	q(Ti)/e	q(L)/e	Bond energy/kJ mol ⁻¹
1 (L = O)	0.0	0.0	1.918	1.453	-0.645	-2587
	10.0	12.4	1.934	1.415	-0.643	-2576
	20.0	27.0	1.955	1.347	-0.636	-2568
	29.9	40.5	1.966	1.312	-0.627	-2571
	30.0	40.6	1.966	1.312	-0.627	-2571
	40.0	57.0	1.986	1.293	-0.616	-2572
	47.0	68.1	2.019	1.286	-0.608	-2568
2 (L = S)	0.0	0.0	2.486	1.103	-0.144	-2127
	10.0	13.3	2.442	1.062	-0.129	-2149
	20.0	26.9	2.422	1.017	-0.104	-2176
	30.0	41.2	2.414	1.002	-0.094	-2197
	32.5	44.9	2.415	0.999	-0.089	-2204
	40.0	56.9	2.424	1.021	-0.096	-2201
	47.0	69.1	2.457	1.060	-0.103	-2190
3 (L = Se)	0.0	0.0	2.634	1.105	-0.104	-2102
	10.0	13.4	2.582	1.014	-0.066	-2124
	20.0	27.5	2.562	1.018	-0.062	-2149
	30.0	42.0	2.554	1.002	-0.051	-2170
	34.5	48.6	2.557	1.003	-0.046	-2179
	40.0	57.2	2.569	1.021	-0.052	-2179
	47.0	68.7	2.605	1.065	-0.065	-2167

orbitals of the three lone pairs of each oxygen atom differ essentially in the nature of hybridization, energy and population (see Table 3). The lone electron pair LP1(O), with minimum energy, corresponds to the hybrid orbital of approximately 54 % s and 46 % p character. LP3(O) with 8 % s and 92 % p character is orientated along the Ti-O axis (see Fig. 5, top left). This indicates a σ -bond between Ti and O. LP3(L) was not detected for **2** and **3**, having a natural Ti-L bond orbital instead. The energies of LP2(O) and LP3(O) on O, with a p electron character of 92–96 %, are ca. 0.3 a.u. higher than that of LP1(O). The populations of the LP2(O) and LP3(O) orbitals are noticeably lower than that of the LP1(O) orbital. Electron density from the three LP orbitals of oxygen is strongly delocalized into the LP* Ti-d orbitals – the occupancy of the oxygen LP orbitals is between 1.62 and 1.95 e.

The Ti-S and Ti-Se bonds of **2** and **3** have a very similar character and population. Figure 5 (bottom row) gives a visualization of the bonding and antibonding Ti-S and Ti-Se NBOs. The interactions between ‘filled’ (donor) Lewis-type NBOs and ‘empty’ (acceptor) non-Lewis NBOs lead to loss of occupancy from the localized NBOs of the idealized Lewis structure into the empty non-Lewis orbitals, and they are referred to as ‘delocalization’ corrections to the zeroth-order natural Lewis structure. The strongest stabilization energy values E(2) (> 65 kJ mol⁻¹) associated with delocalization are summarized in Table 4 for complexes **1–3**. These interactions reflect the electron transference between the orbitals localized in the atoms. The lone pairs LP2(O) and LP3(O) of mainly p character, see Fig. 5 (top row), interact more strongly with the titanium d NBOs than lone pair LP1(O) with

Table 3 The calculated energies, E , and electron populations, $P(> 0.01 e)$, of the bonding (BD) and lone pair (LP) natural bond orbitals (NBOs) for the simplified models **1–3** under a C_s symmetry constraint.

NBO type	1 (L = O)		2 (L = S)		3 (L = Se)	
	P/e	E/a.u.	P/e	E/a.u.	P/e	E/a.u.
BD(Ti - L)	–	–	1.9301 ^a	-0.3108	1.9362 ^b	-0.2934
BD*(Ti - L)	–	–	0.1784	0.1267	0.1751	0.1279
LP*1(Ti)	0.5589	-0.0862	0.5132	-0.0871	0.5075	-0.0868
LP*2(Ti)	0.5137	-0.0706	0.5058	-0.0876	0.4695	-0.0840
LP*3(Ti)	0.5096	-0.0661	0.4518	-0.0858	0.4432	-0.0858
LP*4(Ti)	0.5009	-0.0807	–	–	–	–
LP*5(Ti)	0.4068	-0.0752	–	–	–	–
LP*6(Ti)	0.1559	0.7136	0.2473	0.4178	0.2519	0.3914
LP1(L)	1.9476	-0.5639	1.9665	-0.5870	1.9736	-0.6736
LP2(L)	1.7234	-0.2585	1.6807	-0.1953	1.7099	-0.1829
LP3(L)	1.6247	-0.3040	–	–	–	–
BD(L - C)	1.9826 ^c	-0.8206	1.9717 ^d	-0.5911	1.9652 ^e	-0.5274
BD*(L - C)	0.0275	0.3524	0.0383	0.1827	0.0465	0.1082

^a 25.1 % Ti and 74.9 % S.

^b 26.5 % Ti and 73.5 % Se.

^c 66.4 % O and 33.6 % C.

^d 46.5 % S and 53.5 % C.

^e 43.6 % Se and 56.4 % C.

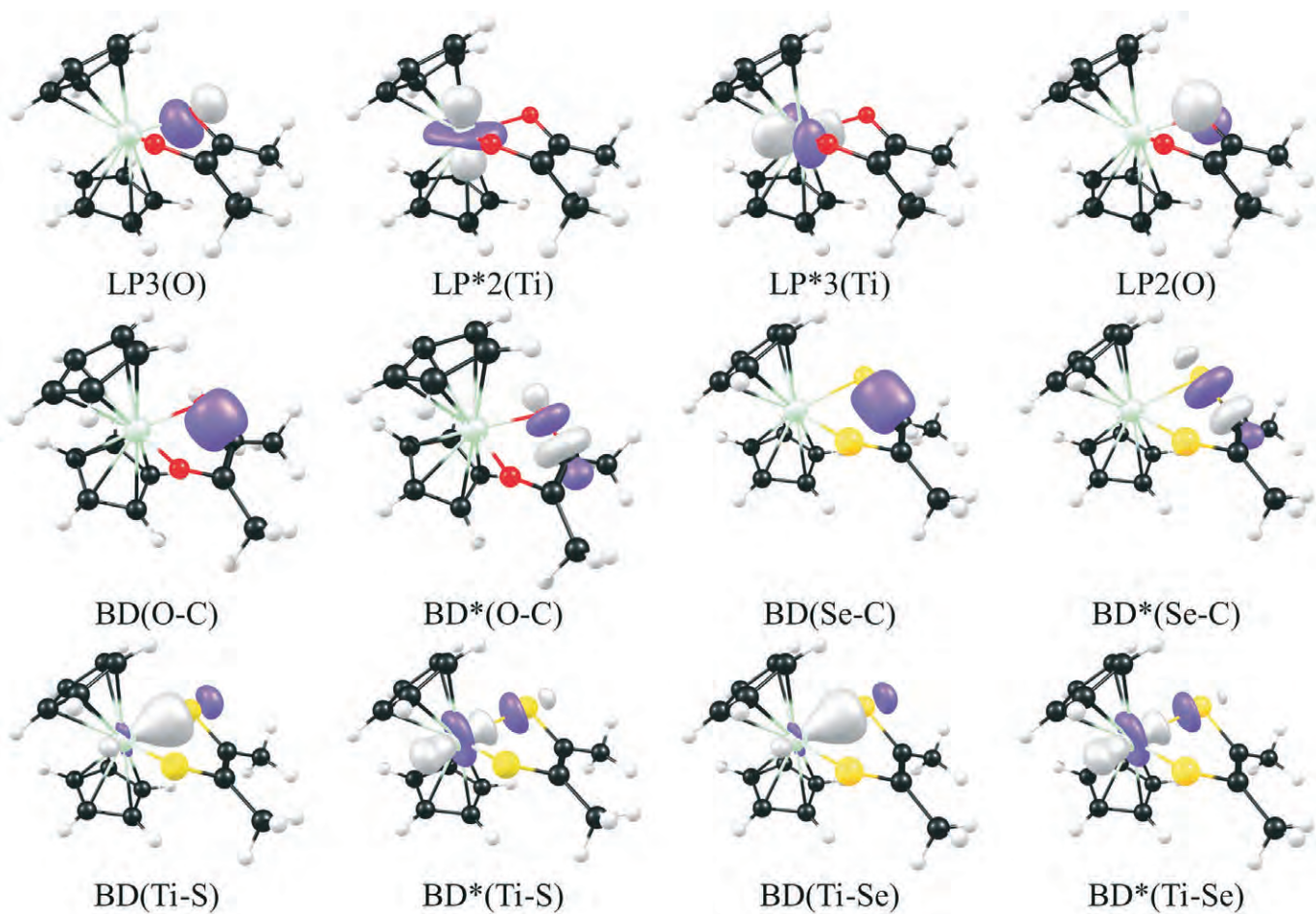


Figure 5 Selected NBOs of the simplified models $\text{Cp}_2\text{Ti}(\text{dioxolene})$ (**1**), $\text{Cp}_2\text{Ti}(\text{dithiolene})$ (**2**) and $\text{Cp}_2\text{Ti}(\text{diselenolene})$ (**3**). A contour of $0.1 \text{ e } \text{\AA}^{-3}$ has been used for the orbital plots. Colour code for atoms: Ti (lime green), C (black), H (white), S (green-yellow) and O (red).

only 46 % p character. The natural bond orbitals $\text{BD}^*(\text{Ti}-\text{S})$ and $\text{BD}^*(\text{Ti}-\text{Se})$ in **2** and **3** interact with a lone pair NBO on Ti of 62–64 % s and 34–37 % p character and electron occupation of 0.25 e^- .

These interactions and the occupancy of the Ti-d orbitals of complexes **1–3** reflect the increase in the electron count of the formal 16-electron $d^0 \text{Cp}_2\text{Ti}^{\text{IV}}(\text{L,L'-BID})$ complexes.

4. Conclusions

$\text{Cp}_2\text{Ti}^{\text{IV}}(\text{L,L'-BID})$ 16-electron d^0 complexes all exhibit a striking structural flexibility in such a way as to increase the electron count by $\text{Ti} \leftarrow \text{L}$ π donation by symmetry lowering and folding of the L,L'-BID ligand around the L...L' axis. Computational evidence of the π -bonding is determined by a natural bond

orbital (NBO) analysis. The out of plane folding angle for maximum $\text{Ti} \leftarrow \text{L}$ π donation increases with larger Ti-L bond lengths: $\text{Cp}_2\text{Ti}^{\text{IV}}(\text{O,O'-BID})$ ($\sim 35^\circ$) < $\text{Cp}_2\text{Ti}^{\text{IV}}(\text{S,S'-BID})$ (47 ° average) < $\text{Cp}_2\text{Ti}^{\text{IV}}(\text{Se,Se'-BID})$ (50 ° average). The bond energies, ΔE , of the Ti-L bonds of complexes $\text{Cp}_2\text{Ti}(\eta^2-\text{SC}(\text{CH}_3)=\text{C}(\text{CH}_3)\text{S})$, **2**, and $\text{Cp}_2\text{Ti}(\eta^2-\text{SeC}(\text{CH}_3)=\text{C}(\text{CH}_3)\text{Se})$, **3**, become stronger (more negative) with increased folding until the point where a steric repulsion between the L,L'-BID and the cyclopentadienyl ligand leads to a weakening in ΔE . The most stable geometries of **2** and **3** have the shortest Ti-L bond lengths and the strongest bonding energies, ΔE , of the Ti-L bond. ΔE as well as the total energy of complex **1** is not very sensitive to the folding angle, θ , between the plane through the Ti-L-L' atoms and the plane through the L'-L-C-C' atoms.

Supplementary Material

A presentation of a number of MOs of the simplified models **1–3**, including the ligand MOs associated with these complexes, and a summary of the optimized Cartesian coordinates of the studied molecules are provided in the supplementary material.

Acknowledgements

Financial assistance by the South African National Research Foundation, under grant number 2067416, and the Central Research Fund of the University of the Free State is gratefully acknowledged.

References and Notes

- N.J. Long, *Metallocenes: an Introduction to Sandwich Complexes*, Blackwell Science, London, UK, 1998, pp. 23, 148–154.

Table 4 Interaction energy, E , between donor and acceptor orbitals for the simplified models **1–3** under a C_s symmetry constraint. Only values $> 65 \text{ kJ mol}^{-1}$ are tabulated.

Complex	Donor NBO	Acceptor NBO	$E/\text{kJ mol}^{-1}$
1	LP3(O)	LP*2(Ti)	214.6
	LP3(O)	LP*3(Ti)	97.3
	LP2(O)	LP*3(Ti)	69.1
	LP*6(Ti)	RY*3(O)	68.1
2	BD*(Ti-S)	LP*6(Ti)	292.7
3	BD*(Ti-Se)	LP*6(Ti)	328.1

- 2 (a) A. Kuhn, A. Muller and J. Conradie, *Polyhedron*, 2009, **28**, 966–974;
(b) E. Erasmus, J Conradie, A. Muller and J.C. Swarts, *Inorg. Chim. Acta*, 2007, **360**, 2277–2283; (c) Z. Gao, C. Zhang, M. Dong, L.Gao, G. Zhang, Z. Liu, G.Wang and D. Wu, *Appl. Organomet. Chem.*, 2006, **20**, 117–124; (e) M. Casado, J.J. Perez-Torrente, M.A. Ciriano, A.J. Edwards, F.J. Lahoz and L.A. Oro, *Organometallics*, 1999, **18**, 5299–5310; (f) F. Hampel, N. van Eikema Hommes, S. Hoops, F. Maaref and R. Schobert, *Eur. J. Inorg. Chem.*, 1998, 1253–1263; (g) P.C. Wailes, R.S.P. Coutts and H. Weigold, *Organometallic Chemistry of Titanium, Zirconium and Hafnium*, Academic Press, New York, NY, USA, 1974.
3. (a) I. Fleming, *Frontier Orbitals and Organic Chemical Reactions*, Wiley, New York, NY, USA, 1976; (b) K. Fukui, *Topics Curr. Chem.*, 1970, **15**, 1–85; (c) G. Klopman, *J. Am. Chem. Soc.*, 1968, **90**, 223–234.
- 4 J.W. Lauher and R. Hoffmann, *J. Am. Chem. Soc.*, 1976, **98**, 1729–1742.
- 5 F. Guyon, M. Fourmigue, P. Audebert and J. Amaudrut, *Inorg. Chim. Acta*, 1995, **239**, 117–124.
- 6 (a) L.C. Song, P.C. Liu, C. Han and Q.M. Hu, *J. Org. Chem.*, 2002, **648**, 119–125; (b) J. Conradie, *Int. J. Quantum Chem.* 2009, **110**, 1100–1107.
- 7 O. Jeannin, M. Nomura and M. Fourmigué, *J. Organomet. Chem.*, 2007, **692**, 4113–4118.
- 8 W. Koch and M.C. Holthausen, *Chemist's Guide to Density Functional Theory*, Wiley-VCH, Weinheim, Germany, 2001 (<http://www3.interscience.wiley.com/cgi-bin/bookhome/86513314>). Accessed 25 July 2009.
- 9 M.J. Frisch, G.W. Trucks, H.B. Schlegel, G.E. Scuseria, M.A. Robb, J.R. Cheeseman, J.A. Montgomery, Jr., T. Vreven, K.N. Kudin, J.C. Burant, J.M. Millam, S.S. Iyengar, J. Tomasi, V. Barone, B. Mennucci, M. Cossi, G. Scalmani, N. Rega, G.A. Petersson, H. Nakatsuji, M. Hada, M. Ehara, K. Toyota, R. Fukuda, J. Hasegawa, M. Ishida, T. Nakajima, Y. Honda, O. Kitao, H. Nakai, M. Klene, X. Li, J.E. Knox, H.P. Hratchian, J.B. Cross, V. Bakken, C. Adamo, J. Jaramillo, R. Gomperts, R.E. Stratmann, O. Yazyev, A.J. Austin, R. Cammi, C. Pomelli, J.W. Ochterski, P.Y. Ayala, K. Morokuma, G.A. Voth, P. Salvador, J.J. Dannenberg, V.G. Zakrzewski, S. Dapprich, A.D. Daniels, M.C. Strain, O. Farkas, D.K. Malick, A.D. Rabuck, K. Raghavachari, J.B. Foresman, J.V. Ortiz, Q. Cui, A.G. Baboul, S. Clifford, J. Cioslowski, B.B. Stefanov, G. Liu, A. Liashenko, P. Piskorz, I. Komaromi, R.L. Martin, D.J. Fox, T. Keith, M.A. Al-Laham, C.Y. Peng, A. Nanayakkara, M. Challacombe, P.M.W. Gill, B. Johnson, W. Chen, M.W. Wong, C. Gonzalez and J.A. Pople, GAUSSIAN 03, Rev. C.02, Gaussian, Inc., Wallingford, CT, USA, 2004.
- 10 J.P. Perdew, J.A. Chevary, S.H. Vosko, K.A. Jackson, M.R. Pederson, D.J. Singh and C. Fiolhais, *Phys. Rev. B*, 1992, **46**, 6671–6687. *Erratum:* J.P. Perdew, J.A. Chevary, S.H. Vosko, K.A. Jackson, M.R. Pederson, D.J. Singh and C. Fiolhais, *Phys. Rev. B*, 1993, **48**, 4978.
- 11 G.A. Zhurko and D.A. Zhurko, Chem Craft, Version 1.6 (build 294), 2008.
- 12 E.D. Glendening, J.K. Badenhoop, A.E. Reed, J.E. Carpenter, J.A. Bohmann, C.M. Morales, and F. Weinhold, NBO 3.1 (Theoretical Chemistry Institute, University of Wisconsin, Madison, WI, USA, 2001).
- 13 W.J. Hehre, *A Guide to Molecular Mechanics and Quantum Chemical Calculations*, Wavefunction Inc., Irvine, CA, USA, 2003, pp. 153,181.
- 14 J.A. Martinho Simoes and J.L. Beauchamp, *Chem. Rev.*, 1990, **90**, 629–688.
- 15 H. Jacobsen, A. Correa, C. Costabile and L. Cavallo, *J. Organomet. Chem.*, 2006, **691**, 4350–4358.
- 16 In order to access the extent of donated and/or backdonated charges, single point calculations for the ligand and the metallic fragment with their frozen geometry in the complex were done. The increase in the natural charge on L and the decrease of the natural charge on Ti gave the same results as above: increase in the natural charge on L: $0.227\text{ e}(\text{O}) < 0.555\text{ e}(\text{S}) < 0.586\text{ e}(\text{Se})$, decrease in the natural charge on Ti: $0.230\text{ e}(\text{O}) < 0.527\text{ e}(\text{S}) \approx 0.520\text{ e}(\text{Se})$.
- 17 Electronegativities on the Pauling scale: 3.44 (O), 2.58 (S) and 2.55 (Se) and 2.55 (C). From <http://en.wikipedia.org/wiki/Electronegativity>. Accessed 25 July 2009.
- 18 A. Kutoglu, *Z. Anorg. Allgem. Chem.*, 1972, **390**, 195–209.
- 19 A. Kutoglu, *Acta Cryst.*, 1973, **B29**, 2891–2897.
- 20 F. Guyon, C. Lenoir, M. Fourmigue, J. Larsen and J. Amaudrut, *Bull. Soc. Chim. France*, 1994, **131**, 217–226.
- 21 S. Vincendeau, V. Colliere and C. Faulmann, *Acta Cryst.*, 2003, **E59**, m268–m270.